Available online at www.sciencedirect.com

ScienceDirect

journal homepage: www.elsevier.com/locate/he

Effect of titanium suboxides on the reaction mechanism of hydrogen-reduced ilmenite

Han Yu [a,b], *Chen Li* [b,c], *Kuixian Wei* [b,c,*], *Yang Li* [d,**], *Wenhui Ma* [a,b,c]

[a] *State Key Laboratory of Complex Nonferrous Metal Resources Clean Utilization, Kunming University of Science and Technology, Kunming 650093, China*

[b] *National Engineering Research Center of Vacuum Metallurgy, Kunming University of Science and Technology, Kunming 650093, China*

[c] *Faculty of Metallurgical and Energy Engineering, Kunming University of Science and Technology, Kunming 650093, China*

[d] *Center for Lunar and Planetary Science, Institute of Geochemistry, Chinese Academy of Sciences, Guiyang 550081, China*

HIGHLIGHTS

- The mechanism of hydrogen reduction of ilmenite is expounded.
- Stable existence of titanium suboxides at reaction temperatures exceed 1100 K.
- Titanium suboxides can reduce ilmenite is confirmed.
- The metallization rate can be increased by holding operation.

ARTICLE INFO

Article history:
Received 18 August 2022
Received in revised form
29 September 2022
Accepted 10 October 2022
Available online 30 October 2022

Keywords:
Hydrogen reduction
Ilmenite
Titanium suboxides
Thermodynamic analysis
Validation experiments

ABSTRACT

Hydrogen metallurgy, as a green metallurgical technology, is one of the effective ways to reduce carbon emissions. The generation of titanium suboxides (Ti_nO_{2n-1}, $3 \leq n \leq 9$) during the hydrogen reduction of ilmenite results in abundant hydrogen and heat loss. In this study, the ability of titanium suboxides to reduce ilmenite is systematically analyzed and confirmed. Thermodynamic calculations reveal that these titanium suboxides exist stably and reduce ilmenite when the reaction temperature exceeds 1100 K. Validation experiments indicate that Ti_3O_5 can be used to reduce ilmenite to iron and rutile. Furthermore, by controlling the reduction time and holding operation in an inert atmosphere, the discovery of metallic iron particles generated inside unreacted ilmenite. This shows that titanium suboxides can reduce ilmenite, and also the metallization rate of iron is increased. This study has great guideline significance for the clean and green production of ilmenite.

* *Corresponding author*. National Engineering Research Center of Vacuum Metallurgy, Kunming University of Science and Technology, Kunming 650093, China.
** *Corresponding author*.
E-mail addresses: kxwei2008@hotmail.com (K. Wei), liyang@mail.gyig.ac.cn (Y. Li).

https://doi.org/10.1016/j.ijhydene.2022.10.071

Introduction

With the progress of China's carbon peak and carbon neutrality targets and related actions, high-quality and low-carbon reforms in the metallurgical industry have become an inevitable trend [1–3]. Hydrogen energy is regarded as the green energy with the most development potential in the 21st century, which has many advantages such as abundant sources, clean and low-carbon, renewable, and a high reduction efficiency [4–8]. Hydrogen metallurgy uses hydrogen as a reducing agent instead of a carbon-based reducing agent, which decreases CO_2 emissions and ensures the green and sustainable development of the metallurgy industry [6,9,10]. Ilmenite is the main raw material for the production of titanium and titanium alloys [11–13]. In a conventional process, the direct smelting of ilmenite is mainly carried out in an electric arc furnace with a carbon-based reducing agent to produce pig iron and titanium-enriched slag. This consumes large amounts of energy and also emits large quantities of CO_2, resulting in severe environmental pollution [14–17]. On the contrary, the direct reduction of ilmenite by hydrogen has a fast reaction rate, low impurity content of the products, and the tail gas produced that is water vapor does not emit pollution into the atmosphere and can achieve zero CO_2 emissions [18–21].

There are many studies related to hydrogen-reduced ilmenite. Zhao and Shadman [22] and Vijay et al. [23] studied the reaction kinetics and mechanism of the hydrogen reduction of ilmenite and concluded that the whole reduction reaction proceeded through three stages: induction stage, acceleration stage, and deceleration stage. By increasing the reaction temperature and hydrogen concentration, during the hydrogen reduction of ilmenite, the reduction rate and reduction degree were also promoted [24–27]. Meanwhile, reducing the grains size also helped increase the contact area of gas, thus accelerating the reaction rate [28,29]. However, upon increasing the reaction temperature, impurities such as MgO, MnO, and SiO_2 gathered at the reaction interface to form an impurity-enriched region that reduced the activity of Fe^{2+} and ultimately reduced the reduction degree of the entire ilmenite sample [15,26,30]. Furthermore, related studies have indicated that the thermodynamic and kinetic conditions of ilmenite can be improved by pre-oxidation treatment [14,31,32]. The initial reduction temperature and apparent activation energy can be reduced during the reduction reaction [14,33]. This is because many micropores, protrusions, and cracks appear on the surface of pre-oxidized ilmenite, which helps increase the gas contact area and improves the reaction rate [34–36]. Dang [17] and Zhang et al. [28] discovered that during the hydrogen reduction of ilmenite, when the reaction temperature was higher than 1220 K, the reduction degree of ilmenite obtained by thermogravimetric analysis was greater than 1. They attributed this to the reduction of rutile that produced Ti_3O_5, causing increased oxygen loss. Obviously, the formation of Ti_3O_5 consumes a large amount of hydrogen. Xu et al. [37] concluded that the reaction activity of plasma hydrogen gradually increased with the reaction temperature during the hydrogen plasma reduction of rutile, which caused rutile to be reduced step-by-step to produce the Magnéli phase (Ti_nO_{2n-1}, $4 \leq n \leq 9$), and relatively stable Ti_3O_5 and Ti_2O_3 phases.

Although there have been many studies on the hydrogen reduction of ilmenite, the main focus of these papers has been the reaction kinetics, phase transformation, impurity migration and strengthening reduction. Apparently, the role of titanium suboxides generated at high temperatures on the reduction of hydrogen-reduced ilmenite can reduce ilmenite is not given a clear explanation. The purpose of this paper is to examine in detail the existence conditions of titanium suboxides and their influence on the overall reduction reaction mechanism on hydrogen reduction of ilmenite concentrate, which is of great significance to complement and improve the understanding of the mechanism.

Materials and experimental methods

Materials and analysis

The ilmenite concentrate was obtained from an iron and steel plant, and its chemical composition is shown in Table 1, in which the main oxides are TiO_2, FeO, SiO_2 and Al_2O_3. In Fig. 1, the XRD analysis indicates that phase compositions of raw materials include ilmenite ($FeTiO_3$) with a small amount of rutile (TiO_2) and pseudobrookite ($FeTi_2O_5$). The ilmenite concentrate was ground and sieved to a particle size fraction

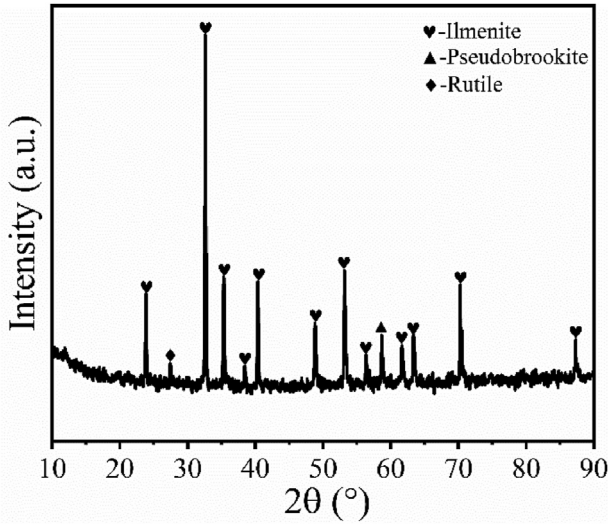

Fig. 1 – XRD pattern of ilmenite concentrate.

Table 1 – Chemical composition of ilmenite concentrate (wt. %).

Total Fe	TiO_2	FeO	SiO_2	Al_2O_3	Fe_2O_3	MgO	CaO	MnO
31.70	41.48	38.29	10.86	4.20	2.74	1.95	0.61	0.45

of (100 ± 30) μm. High-purity hydrogen (99.999 vol%) was used as the reducing agent, and pure argon (99.99 vol%) was used as the protective gas.

Experimental procedure

Isothermal reduction experiments were carried out in a hydrogen reduction furnace (horizontal tube furnace). The schematic of the experimental device is presented in Fig. 2, in which the heating components were silicon carbon rods, and the temperature control accuracy was ±1 K. The sieved ilmenite concentrate powder and corundum boat were put into a vacuum-drying oven separately and kept under vacuum at 373 K for 8 h to remove the moisture. After drying, the corundum boat containing the sample was placed in the central heating zone of the furnace tube. To ensure that the furnace tube was in an oxygen-free environment throughout the experiment, three gas washings were performed, and then pure argon gas was injected for protection. The heating process adopted a segmented heating procedure (T_1: 273–473 K, heating rate: 5 K min^{-1}; T_2: 473–1473 K, heating rate: 10 K min^{-1}). When the temperature in the furnace reached the experimental temperature, the argon gas inlet valve was closed, and then the hydrogen gas inlet valve was opened. The gas flow rate was set to 200 ml/min. The remaining H_2 and H_2O generated during the reaction were discharged through the gas outlet. To detect whether hydrogen leaked during the whole reduction reaction, a fixed hydrogen detector was used to detect each interface. After the reaction was finished, the hydrogen was cut off, and then argon gas was injected for protection and cooling. When the temperature in the furnace reached room temperature, the sample was taken out.

Characterization

The chemical composition of the ilmenite concentrate was obtained by X-ray fluorescence spectrometry (XRF, ZKS100e, Japan). The phase compositions of the experimental samples were investigated by X-ray diffraction (XRD, D8Advance, Bruker, Germany). Thermogravimetric-differential thermal analyses were performed in a thermal analyzer (TG-DTA, STA449F3, NETESCH, Germany). The microstructure of the samples was observed using a field emission scanning electron microscope equipped with X-ray energy-dispersive spectroscopy (FESEM-EDS, Hillsboro, OR, FEI, USA). The metallization rate of the reduced samples was measured by chemical titration (GB/T 38812.2-2020, China) and can be expressed as Eq. (1):

$$Metallization\ rate = \frac{Fe^0}{TFe} \times 100\% \quad (1)$$

where Fe^0 and TFe represent the mass fraction of metallic iron and the total iron in the reduced ilmenite sample, respectively [38].

Analysis and discussion

Thermodynamic analysis

The thermodynamic equilibrium of a chemical reaction in a closed system was calculated in accordance with the Second Law of Thermodynamics [39]. The standard Gibbs free energy diagram of the involved Eqs. (2)–(8) that varying with temperature, and the dominant region diagram of the $FeO–TiO_2–O_2$ system were obtained using relevant thermodynamic calculations (HSC 6.0) and phase diagram analysis (FactSage 8.0) respectively, as shown in Fig. 3.

The relevant chemical equations were as follows:

$$H_2(g) + FeTiO_3(s) \rightarrow Fe(s) + TiO_2(s) + H_2O(g) \quad (2)$$

$$H_2(g) + 5/6FeTiO_3(s) \rightarrow 5/6Fe(s) + 1/6Ti_5O_9(s) + H_2O(g) \quad (3)$$

$$H_2(g) + 3/4FeTiO_3(s) \rightarrow 3/4Fe(s) + 1/4Ti_3O_5(s) + H_2O(g) \quad (4)$$

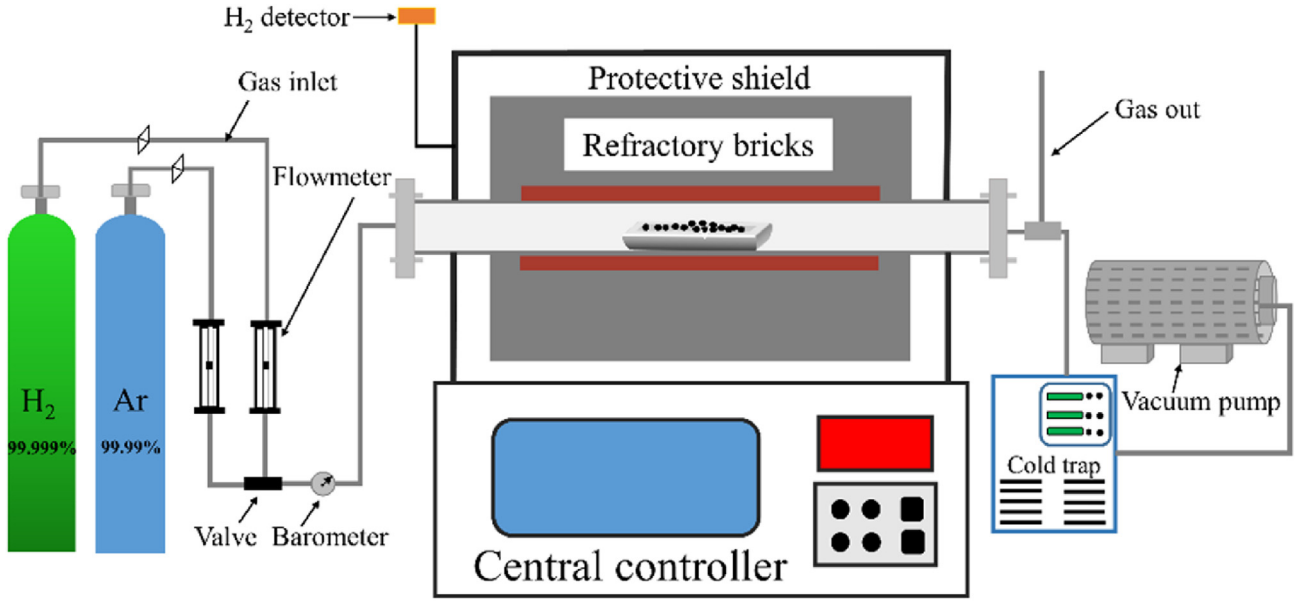

Fig. 2 – Schematic apparatus of the hydrogen reduction furnace.

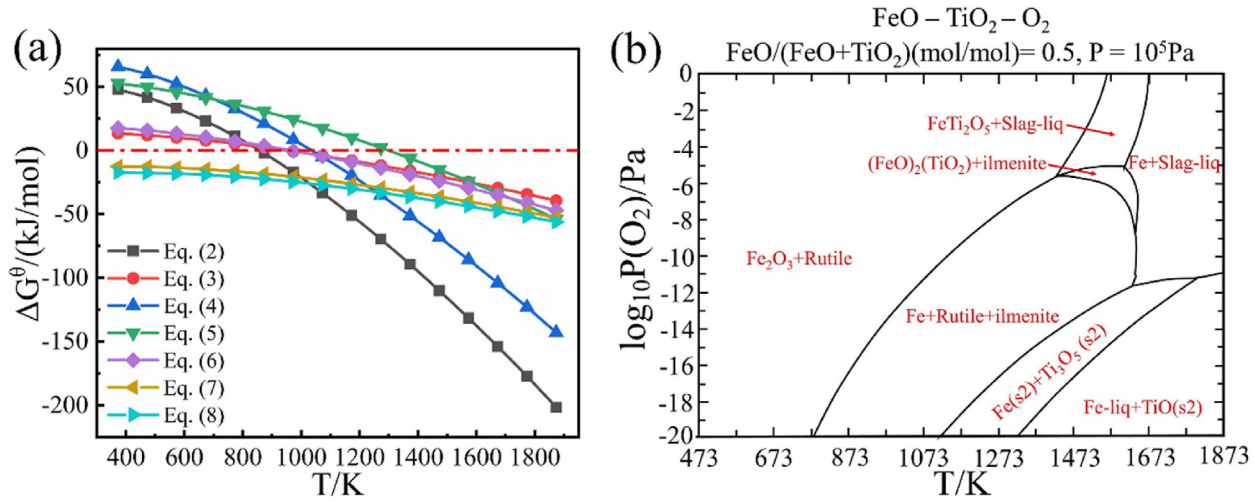

Fig. 3 – Thermodynamics analysis: (a) standard Gibbs free energy of different hydrogen reduction temperatures of the ilmenite, Eqs. (2)–(8); (b) stable phase diagram of the $FeO–TiO_2 – O_2$ system.

$$H_2(g) + 2FeTiO_3(s) \rightarrow Fe(s) + FeTi_2O_5(s) + H_2O(g) \quad (5)$$

$$H_2(g) + 3/5FeTi_2O_5(s) \rightarrow 3/5Fe(s) + 2/5Ti_3O_5(s) + H_2O(g) \quad (6)$$

$$Ti_5O_9(s) + FeTiO_3(s) \rightarrow Fe(s) + 6TiO_2(s) \quad (7)$$

$$Ti_3O_5(s) + FeTiO_3(s) \rightarrow Fe(s) + 4TiO_2(s) \quad (8)$$

In Fig. 3(a), It is found that when the reaction temperature is above 852 K, the standard Gibbs free energy of Eq. (2) is $\Delta G^{\theta}_{852K} < 0$, where ilmenite begins to be reduced by hydrogen. The obtained products are H_2O, Fe, and TiO_2. When the temperature is above 1100 K, the standard Gibbs free energy gradually decreases. Therefore, TiO_2 in the products is gradually reduced to form the Magnéli phase and Ti_3O_5, representing Eqs. (3) and (4). When the temperature is higher than 1273 K, $FeTi_2O_5$ is generated first, and then $FeTi_2O_5$ is continuously reduced by hydrogen. Finally, Fe, Ti_3O_5, and H_2O are generated, representing Eqs. (5) and (6). However, it is worth noting that these titanium suboxides and ilmenite can undergo a reduction reaction to generate TiO_2 and Fe, as shown by Eqs. (7) and (8).

According to the experimental conditions and the molar ratio of FeO: TiO_2 = 1: 1 in ilmenite ($FeO{\cdot}TiO_2$) [23], the pressure ($P = 10^5$ Pa) and $FeO/(FeO + TiO_2) = 0.5$ were set in the $FeO–TiO_2 – O_2$ phase diagram. In the $FeO–TiO_2 – O_2$ phase diagram, as the temperature of the system increases and the partial pressure of oxygen decreases, the rutile phase gradually transforms into titanium suboxides. When the temperature is in the range of 1100–1673 K, a stable Ti_3O_5 phase exists in the system, as shown in Fig. 3(b).

Through thermodynamic calculations and phase diagram analysis, it was found that titanium dioxide was gradually reduced by hydrogen when the reaction temperature was higher than 1100 K. Finally, a series of titanium suboxides (Magnéli phase and Ti_3O_5) were generated, which could reduce ilmenite. It was manifested that these titanium suboxides could promote the reduction of ilmenite together with hydrogen, thus changing the reaction path of hydrogen reduction of ilmenite.

Phase transformation analysis

Based on the thermodynamic analysis, the reaction temperature of hydrogen reduction ilmenite concentrate powder in this experiment was 1073–1373 K. The phase transformation of the samples under different reduction conditions was characterized by XRD analysis, and the results are shown in Fig. 4.

In Fig. 4(a), when the reduction temperature is 1073 K and the reduction time is 40 min, the diffraction peaks of ilmenite disappear, and only the diffraction peaks of iron and rutile are present, indicating that the iron oxides in ilmenite concentrate are completely reduced by hydrogen to produce metal iron. When the reaction temperatures are 1173 and 1273 K and the reduction times are 30 min and 20 min, respectively, the products are mainly composed of ilmenite, iron, and rutile. Moreover, the intensity of the diffraction peaks of ilmenite gradually decreases upon increasing the reaction temperature, while the diffraction peaks of iron and rutile are gradually broadened and the intensity is also gradually increased. When the reaction temperature is 1373 K and the reduction time is 20 min, the diffraction peaks of pseudobrookite appear in addition to iron and rutile. However, in the XRD patterns of the samples reduced by hydrogen under the above experimental conditions, titanium oxides exist only in the form of rutile, but the Magnéli phase and Ti_3O_5 have not yet appeared.

The results of the phase analysis at a reduction time of 60 min and at reaction temperatures of 1173, 1273, and 1373 K are shown in Fig. 4(b). When the reduction temperature is 1173 K, the diffraction peaks of iron and rutile and a small amount of the Magnéli phase diffraction peaks appear. When the reduction temperature increases to 1273 K, the diffraction peak of rutile disappears, and the phase compositions are iron, Magnéli phase and Ti_3O_5. The diffraction peak of the Magnéli phase disappears when the reduction temperature is

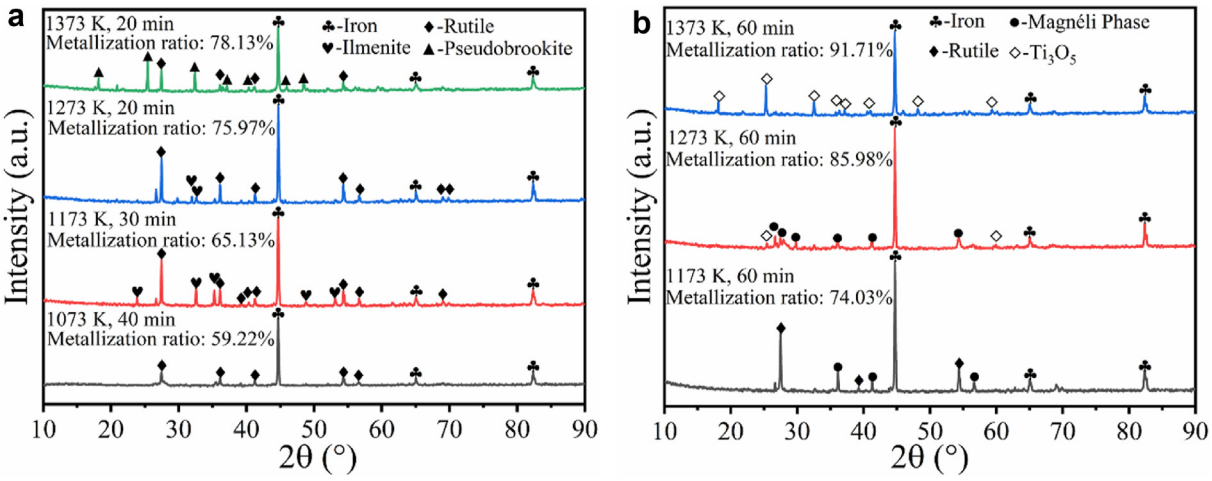

Fig. 4 – XRD patterns of hydrogen-reduced ilmenite under different conditions: (a) hydrogen reduction at a reaction temperature of 1073–1373 K for 40–20 min; (b) hydrogen reduction at a reaction temperature of 1173–1373 K for 60 min.

increased to 1373 K, and the phase compositions are only iron and Ti_3O_5.

According to the XRD analysis of the samples under different experimental conditions and combined thermodynamic calculation results, it was found that: when the reaction temperature was 852–1100 K, the phase compositions of the products included iron and rutile. When the reduction temperature was raised to 1100–1373 K, it was difficult for the titanium suboxides to exist stably by the short-term hydrogen reduction, which was due to a reduction reaction that occurred between the titanium suboxides and the remaining ilmenite. However, when the hydrogen reduction time was extended to 60 min, ilmenite was completely reduced upon gradually increasing the reaction temperature. During this process, rutile in the products was first reduced by hydrogen to generate the Magnéli phase, and then the Magnéli phase was further reduced by hydrogen to generate Ti_3O_5. In other words, rutile was reduced step-by-step and finally existed as stable Ti_3O_5 upon increasing the reaction temperature, which was consistent with the thermodynamic calculations.

Microstructural analysis of experimental products

To investigate the microstructural characteristics of hydrogen-reduced ilmenite, the ilmenite samples after different reduction conditions were characterized using SEM and EDS, as shown in Fig. 5 and Table 2.

In Fig. 5(a)–(b), many pores are found in the sample. It might have been due to the removal of oxygen atoms from iron oxide and tensile stress, which made the whole particles loose and porous [26,40]. The SEM images clearly show that there are two phases with a significant contrast difference in the products. The single-point EDS analysis (Spots 1–2) indicates that there is an obvious layered structure that is mainly composed of iron and rutile, with iron particles embedded in the rutile matrix. Combined with the XRD analysis (Fig. 4(a)), this shows that the sample completely reduced at 1073 K, but does not produce titanium suboxides. In Fig. 5(c)–(f), the microstructure is similar between the two incompletely-reduced samples. According to the EDS analysis (Spots 3–8), it is detected that the two reduced-samples both consist of three phases with different contrast differences, which are iron, rutile, and ilmenite. Most metallic iron particles are located in the outermost layer of the ilmenite grains and wrapped the whole particle. The rutile layer is located between the iron layer and the ilmenite layer, a small number of iron particles and flake iron filings exist in the rutile layer. Simultaneously, there are many iron particles formed along the crack, demonstrating a strong tendency for iron and rutile to separate in the reduction products. The iron particles diffuse through the rutile layer to the outer layer of the ilmenite grains [22]. This is probably due to the fact that during the hydrogen reduction ilmenite reaction, the nascent iron particles have a high surface energy and chemical potential. The higher the temperature, the higher their surface energy and chemical potential. The nascent metallic iron particles diffuse and converge to eventually form larger layered metallic iron, thereby reducing the surface energy and eventually reaching a stable state.

In Fig. 5(g)–(h), the composition and distribution of the phases in the sample are identified to be different from those in Fig. 5(c) and (e). Combined with the EDS (Spots 9–11) and XRD analysis (Fig. 4(a)), it is noticed that the metallic iron particles do not converge in the outermost layer of the ilmenite grain, eventually emerging in the iron layer, but are instead embedded in the rutile matrix. The unreacted phase in the grains is pseudobrookite. However, as indicated in the above EDS analysis results (Spots 4, 7, and 10), there is a phenomenon in which the oxygen atoms are lost in the rutile layer at the reaction interface when the reduction temperatures are higher than 1100 K. This illustrates that these titanium suboxides generated during high-temperature reduction may exist in the rutile layer.

Behavior analysis of Ti_3O_5 during reduction process

According to the thermodynamic calculations and XRD analysis of hydrogen-reduced ilmenite, it was found that rutile

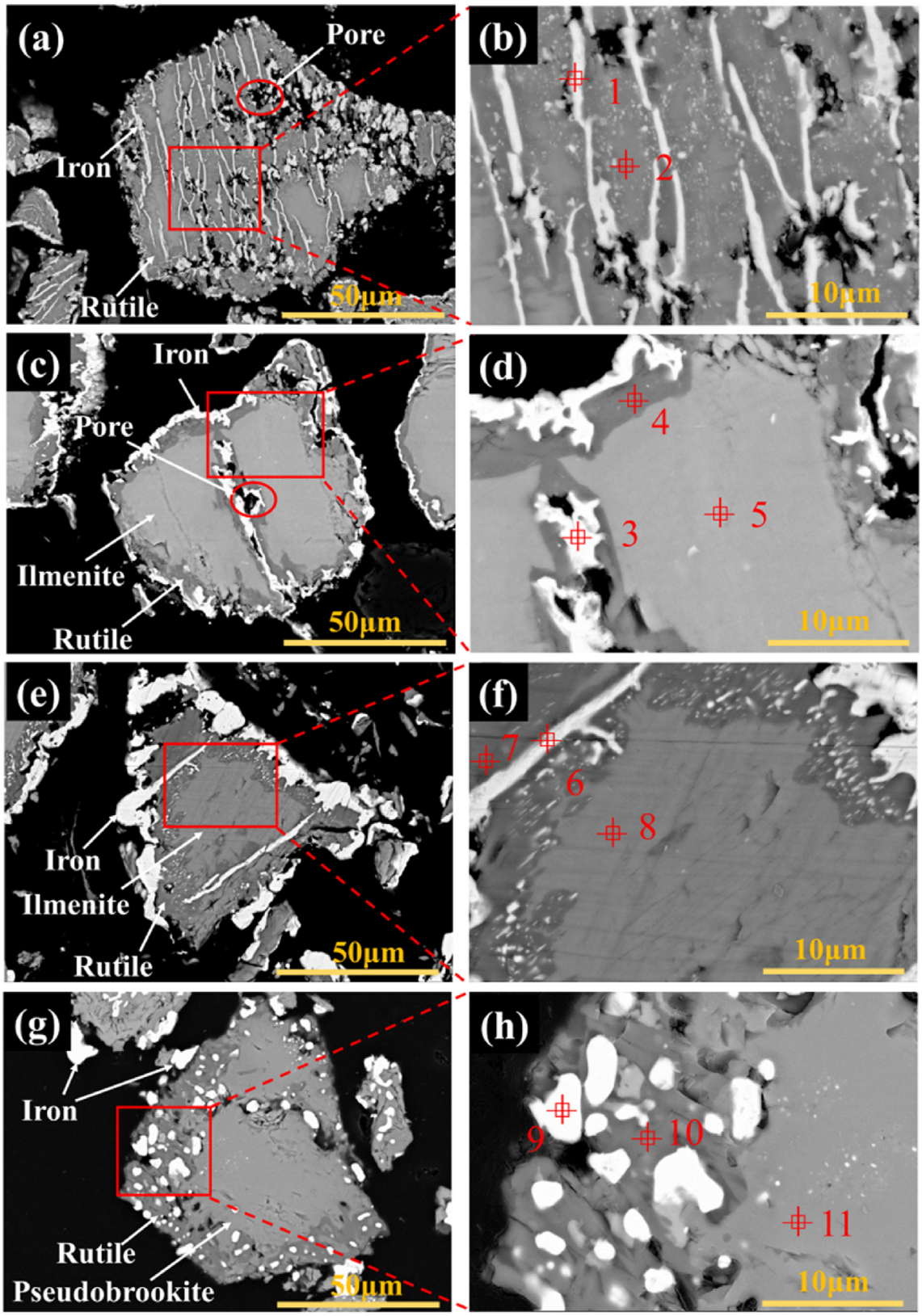

Fig. 5 – Cross-section SEM images and EDS analysis of hydrogen-reduced ilmenite under different conditions: (a)–(b) T: 1073 K, t: 40 min; (c)–(d) T: 1173 K, t: 30 min; (e)–(f) T:1273 K, t: 20min; (g)–(h) T: 1373 K, t: 20 min (The bright white, dark gray, and light gray parts respectively represent iron, rutile, ilmenite and pseudobrookite.).

Table 2 – EDS point analysis of selected phases in different samples (at. %).

Spot	Element						Fe/Ti	Ti/O	Main Phase
	O	Fe	Ti	Mg	Mn	Total			
1	12.4	77.8	9.8	–	–	100.0	7.94	–	Iron + Rutile
2	62.2	5.5	32.3	–	–	100.0	–	0.52	Rutile
3	5.7	90.4	3.9	–	–	100.0	23.18	–	Iron + Rutile
4	63.7	0.5	35.7	–	–	100.0	–	0.56	Rutile
5	55.0	20.7	22.9	1.0	0.4	100.0	0.90	–	Ilmenite
6	7.3	89.5	3.2	–	–	100.0	27.96	–	Iron + Rutile
7	62.0	1.0	37.0	–	–	100.0	–	0.60	Rutile
8	55.4	17.8	20.5	4.9	1.4	100.0	0.87	–	Ilmenite
9	5.0	91.6	3.4	–	–	100.0	26.94	–	Iron + Rutile
10	61.6	1.6	36.8	–	–	100.0	–	0.60	Rutile
11	55.3	13.0	28.8	2.3	0.6	100.0	0.45	–	Pseudobrookite

was gradually reduced to the Magnéli phase and Ti_3O_5 when the reaction temperature was above 1100 K. Moreover, thermodynamic calculations showed that these titanium suboxides could reduce ilmenite to produce iron and rutile. Therefore, to further reveal the effect of Ti_3O_5 on the reduction process, corresponding verification experiments were conducted.

In this validation experiment, Ti_3O_5 was used as the reducing agent. Ti_3O_5 and ilmenite concentrate were mixed and ground in a molar ratio of 1: 1, placed in a furnace under an argon atmosphere, heated to 1273 K, and held for 60 min. The mixed samples were also subjected to thermogravimetric-differential thermal analysis at a heating rate of 10 K/min. In addition, to further investigate if the titanium suboxides generated in the reaction process could promote the reduction of ilmenite, the hydrogen reduction of ilmenite was carried out at a reaction temperature of 1273 K for 20 min, and then the gas was changed to argon and held for 60 min. The results of its correlation analysis are shown in Figs. 6–7, and Tables 3and4.

The pattern in Fig. 6(a) shows that the products of the Ti_3O_5 reduction of ilmenite are mainly composed of iron and rutile. This indicates that ilmenite can be completely reduced by Ti_3O_5 under these conditions. TG-DTA analysis shows that the overall mass remains almost unchanged throughout the reduction reaction, as shown in Fig. 6(b). Nonetheless, upon gradually increasing the reaction temperature, a large exothermic peak appears in the DTA curve when the temperature is in the range of 600–1400 K. The exothermic peak reaches the maximum at 926.3 K. After that, the exothermic process in the system gradually decreases until the reaction of Ti_3O_5 and ilmenite is completed.

From the above analysis, it could be concluded that when ilmenite concentrate was reduced by hydrogen for a short period of time and the hydrogen supply was stopped, the titanium suboxides generated and unreduced ilmenite during the cooling process continued to underwent reduction reactions to produce iron and rutile, which causing the titanium suboxides were consumed. This could also be explained that in the above experiments of hydrogen-reduced ilmenite, the experimental samples failed to detect the diffraction peaks corresponding to these titanium suboxides by XRD analysis at reaction temperatures of 1173–1373 K and reaction times of 30 and 20 min, respectively. Stable diffraction peaks of the Magnéli phase and Ti_3O_5 could be found in the XRD patterns when the reduction time of hydrogen-reduced ilmenite reached 60 min.

The microstructure and EDS single-point analysis of these verification experiments are shown in Fig. 7(a)–(d) and Table

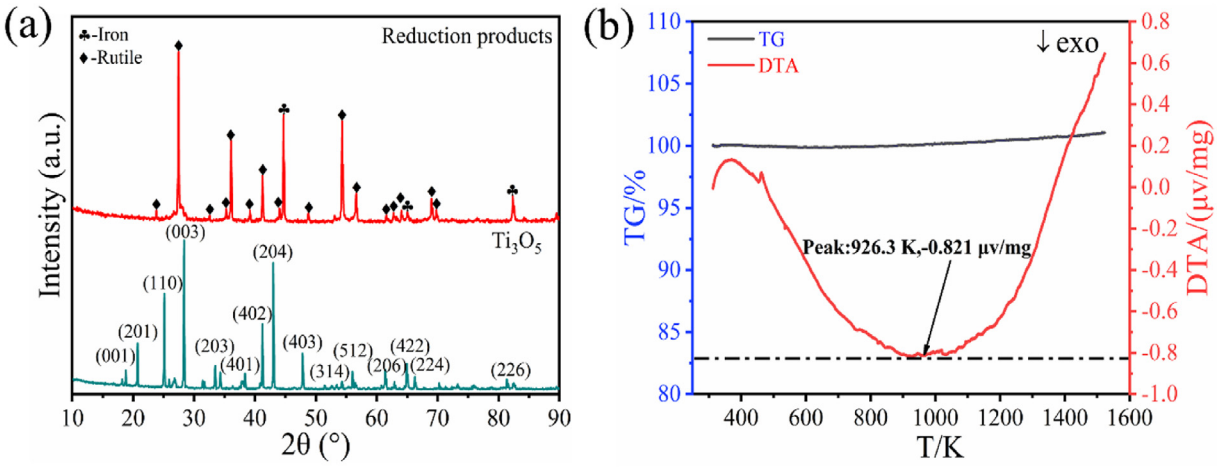

Fig. 6 – XRD pattern and TG/DTA analysis: (a) XRD patterns of Ti_3O_5, products of ilmenite reduced by Ti_3O_5; (b) TG/DTA analysis results of 1: 1 M Ti_3O_5 and ilmenite (exo: exothermic reaction).

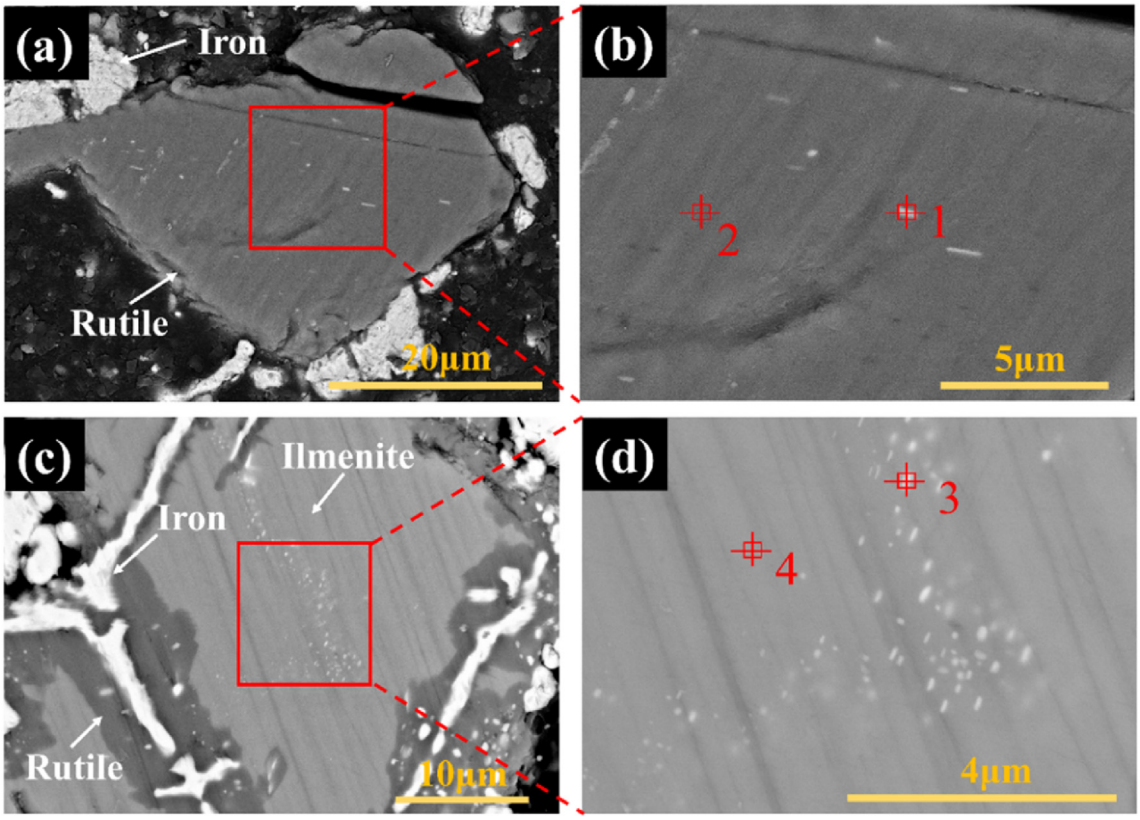

Fig. 7 – SEM images and EDS locations: (a)–(b) ilmenite reduced by Ti_3O_5; (c)–(d) ilmenite reduced by hydrogen at 1273 K for 20 min and then changing into argon holding duration of 60 min.

Table 3 – EDS point analysis of selected phases in different samples (at. %).

Spot	Element						Fe/Ti	Ti/O	Main Phase
	O	Fe	Ti	Mg	Mn	Total			
1	58.3	13.0	28.7	–	–	100.0	0.45	–	Iron + Rutile
2	68.2	–	31.8	–	–	100.0	–	0.47	Rutile
3	55.7	21.8	19.9	1.7	0.9	100.0	1.10	–	Iron + Ilmenite
4	58.2	17.5	21.7	1.6	1.0	100.0	0.81	0.37	Ilmenite

Table 4 – Metallization rates of iron after different holding times for the hydrogen-reduced ilmenite.

sample	Number	Conditions			Metallization Rate/%	Average Metallization Rate/%
		T/K	Reduction time/min	Holding time/min		
1	A	1273	20	0	76.32	75.97
	B	1273	20	0	75.62	
2	C	1273	20	60	85.31	85.17
	D	1273	20	60	85.03	

3. In Fig. 7(a)–(b), the large metallic iron particles are mainly distributed at the edges of the whole grain, and the middle part is rutile after the reaction of the mixed samples at the predetermined temperature. Besides, there are some submicron-sized metallic iron particles in the rutile matrix. This may be because during the reduction of ilmenite by Ti_3O_5, most of the generated metallic iron particles could diffuse to the outside of the reaction interface and eventually accumulate on the whole grain exterior. During the cooling process, however, a small portion of metallic iron particles may have failed to diffuse completely to the exterior due to the deterioration of the kinetics condition and eventually are embedded in the interior of the rutile particles.

In Fig. 7(c)–(d), it is found that the majority of the generated metallic iron particles converge in the outer layer of ilmenite grains, and there are some small nanoparticles iron in the interior of the unreacted ilmenite grains. However, in the sample reduced under the same conditions without a holding

operation, it is difficult to detect metallic iron particles inside by the SEM images, as shown in Fig. 5(e)–(f). The comparative experiment indicated that after the ilmenite is reduced by hydrogen at high a temperature with a short time, and then followed holding operation under an inert atmosphere, these titanium suboxides (Magnéli phase and Ti_3O_5) in the reduction products reacted with the internal unreduced ilmenite via solid-solid reduction reaction. This may be due to the non-stoichiometric amount of oxygen in the titanium suboxide causes oxygen vacancies and Ti^{3+} defects, which has strong catalytic properties and high electrical conductivity [41,42]. These titanium suboxides have the ability to reduce ilmenite to iron and rutile. A small number of metallic iron particles remained in the interior of the ilmenite particles because they may have failed to migrate to the iron-rich phase during the cooling process. Therefore, these generation of titanium suboxides at high temperatures can promote the reduction of ilmenite and thus increase the metallization rate.

The hydrogen reduction of ilmenite powder before and after holding operation was analyzed by chemical titration, as shown in Table 4. The average metallization rate of the samples was 75.79% after hydrogen reduction at 1273 K for 20 min without a holding operation. However, under the same hydrogen reduction conditions, the average metallization rate was 85.17% after the reaction by holding operation, which is a noticeable increase in the relative average metallization rate. This fully indicates that the titanium suboxides generated during the reaction can promote the reduction of the entire ilmenite, thereby improving the metallization rate of iron.

Reaction mechanism

In the whole process of hydrogen reduction of ilmenite, when the reaction temperature was lower than 1100 K, hydrogen diffused to the reaction interface of ilmenite grains and ilmenite underwent a gas-solid reduction reaction to produce iron, rutile, and water vapor. When the reaction temperature was higher than 1100 K, the hydrogen reduction of ilmenite first produced iron, rutile, and water vapor, while hydrogen continuously reduced the rutile generated in the reaction interface to generate the Magnéli phase, which was further reduced to Ti_3O_5. These titanium suboxides generated at the reaction interface and unreacted ilmenite underwent a solid-solid reduction reaction to produce iron and rutile. The generated metallic iron particles migrated and aggregated into the iron-rich phase of the ilmenite grains, while rutile was continuously reduced by hydrogen at the reaction interface to produce titanium suboxides, which, in turn, continued to reduce unreacted ilmenite. Accordingly, the hydrogen reduction of ilmenite at a high-temperature and the overall gas-solid and solid-solid reduction reactions occurred. The generated titanium suboxides promoted the reduction of ilmenite, and also were beneficial to improve the metallization rate. Corresponding to the whole reduction reaction, the schematic diagram of the reaction mechanism is shown in Fig. 8.

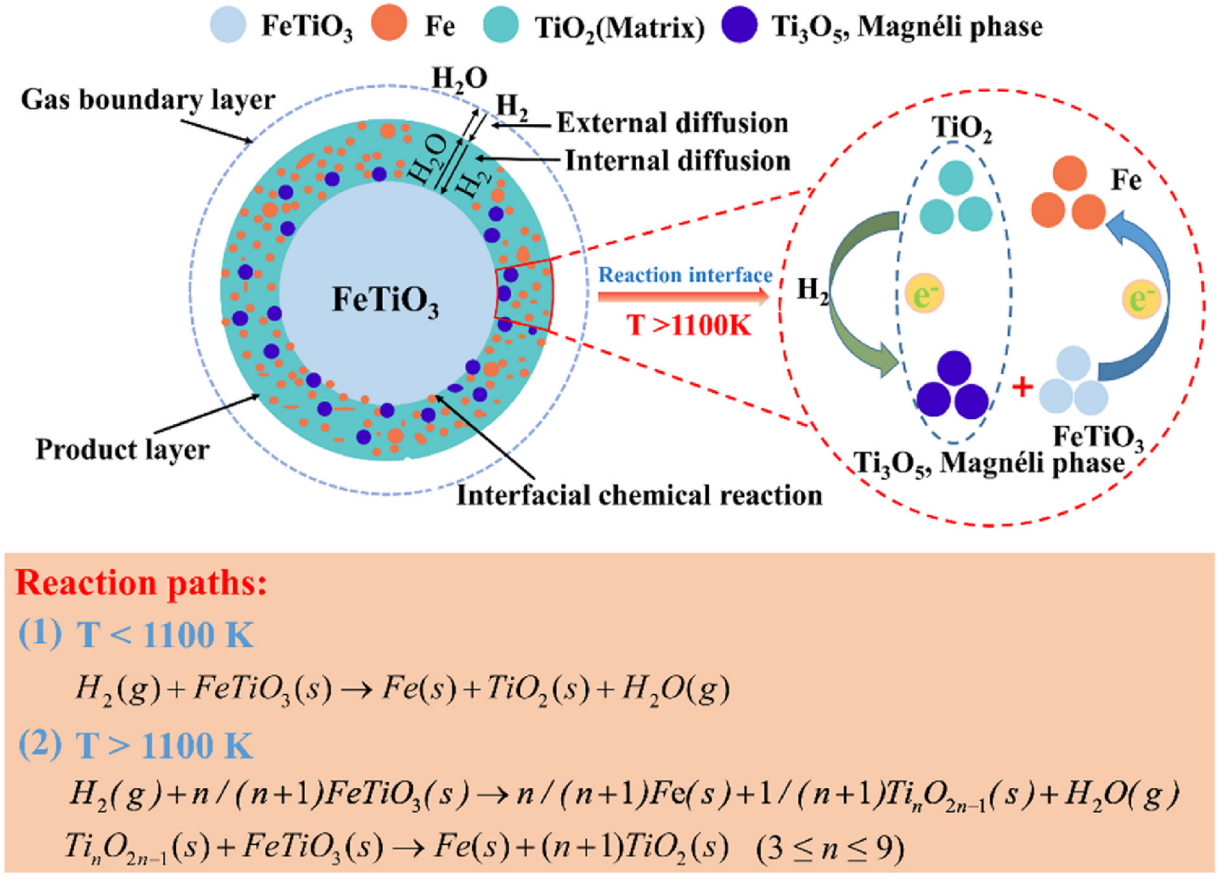

Fig. 8 – The schematic diagram of hydrogen reduction of ilmenite.

Conclusion

According to thermodynamic calculations and experimental results, when the reduction temperature was higher than 1100 K, rutile was first reduced by hydrogen to form the Magnéli phase, and then the Magnéli phase was further reduced by hydrogen to form stable Ti_3O_5. Because these titanium suboxides can synergistically reduce ilmenite with hydrogen, thus the whole reduction reaction occurred via gas-solid and solid-solid reactions. Ilmenite that underwent hydrogen reduction for a short time was kept in an inert atmosphere, and the titanium suboxides could reduce the unreduced ilmenite inside the grains, the metallization rate of iron was increased relative to the sample without holding operation. In conclusion, the rational utilization of titanium suboxides generated in the process of hydrogen reduction of ilmenite can not only reduce the loss of hydrogen and heat, but also improve the metallization rate of iron, which is of great benefit to promote the clean production of ilmenite.

Credit authorship contribution statement

Han Yu: Manuscript, Conceptualization, Methodology, Writing-original draft. Chen Li: English Writing-reviewing. Kuixian Wei: Supervision. Yang Li: Manuscript, Writing-reviewing. Wenhui Ma: Project administration.

Declaration of competing interest

The authors declare that they have no known competing financial interests or personal relationships that could have appeared to influence the work reported in this paper.

Acknowledgments

This study was financially supported by the Yunnan Provincial Outstanding Youth Science Foundation (No. 202101AV070007), the Reserve Talents of Young and Middle-aged Academic and Technical Leaders in Yunnan Province (No.2018HB009).

REFERENCES

[1] Zhang X, Jiao K, Zhang J, Guo Z. A review on low carbon emissions projects of steel industry in the World. J Clean Prod 2021;306. https://doi.org/10.1016/j.jclepro.2021.127259.
[2] Ren L, Zhou S, Peng T, Ou X. A review of CO2 emissions reduction technologies and low-carbon development in the iron and steel industry focusing on China. Renew Sustain Energy Rev 2021;143. https://doi.org/10.1016/j.rser.2021.110846.
[3] Fan Z, Friedmann SJ. Low-carbon production of iron and steel: technology options, economic assessment, and policy. Joule 2021;5:829–62. https://doi.org/10.1016/j.joule.2021.02.018.
[4] Tan N, Li H, Ding Z, Wei K, Ma W, Wu D, et al. Hydrogen generation during the purification of metallurgical-grade silicon. Int J Hydrogen Energy 2021;46:23406–16. https://doi.org/10.1016/j.ijhydene.2020.10.117.
[5] Liu W, Zuo H, Wang J, Xue Q, Ren B, Yang F. The production and application of hydrogen in steel industry. Int J Hydrogen Energy 2021;46:10548–69. https://doi.org/10.1016/j.ijhydene.2020.12.123.
[6] Tang J, Chu M-s, Li F, Feng C, Liu Z-g, Zhou Y-s. Development and progress on hydrogen metallurgy. International Journal of Minerals, Metallurgy and Materials 2020;27:713–23. https://doi.org/10.1007/s12613-020-2021-4.
[7] Dawood F, Anda M, Shafiullah GM. Hydrogen production for energy: an overview. Int J Hydrogen Energy 2020;45:3847–69. https://doi.org/10.1016/j.ijhydene.2019.12.059.
[8] Li F, Chu M, Tang J, Liu Z, Guo J, Yan R, et al. Thermodynamic performance analysis and environmental impact assessment of an integrated system for hydrogen generation and steelmaking. Energy 2022;241. https://doi.org/10.1016/j.energy.2021.122922.
[9] Vogl V, Åhman M, Nilsson LJ. Assessment of hydrogen direct reduction for fossil-free steelmaking. J Clean Prod 2018;203:736–45. https://doi.org/10.1016/j.jclepro.2018.08.279.
[10] Klimova V, Pakhaluev V, Shcheklein S. On the problem of efficient production of hydrogen reducing gases for metallurgy utilizing nuclear energy. Int J Hydrogen Energy 2016;41:3320–5. https://doi.org/10.1016/j.ijhydene.2015.12.148.
[11] He C, Zheng C, Dai W, Fujita T, Zhao J, Ma S, et al. Purification and phase evolution mechanism of titanium oxycarbide (TiCxOy) produced by the thermal reduction of ilmenite. Minerals 2021;11. https://doi.org/10.3390/min11020104.
[12] Yunos NFM, Chong JH, Mohammed AI, Idris MA. Phase evolution during carbothermal reduction of langkawi ilmenite ore at different reaction times. Mater Sci Forum 2020;1010:391–6. https://doi.org/10.4028/www.scientific.net/MSF.1010.391.
[13] Lv W, Lv X, Xiang J, Zhang Y, Li S, Bai C, et al. A novel process to prepare high-titanium slag by carbothermic reduction of pre-oxidized ilmenite concentrate with the addition of Na2SO4. Int J Miner Process 2017. https://doi.org/10.1016/j.minpro.2017.08.004. S0301751617301783.
[14] Lv W, Lv X, Xiang J, Hu K, Zhao S, Dang J, et al. Effect of preoxidation on the reduction of ilmenite concentrate powder by hydrogen. Int J Hydrogen Energy 2019;44:4031–40. https://doi.org/10.1016/j.ijhydene.2018.12.139.
[15] Chang-Yuan LU, Zou XL, Xiong-Gang LU, Xie XL, Zheng K, Xiao W, et al. Reductive kinetics of Panzhihua ilmenite with hydrogen. Trans Nonferrous Metals Soc China 2016;26:3266–73. https://doi.org/10.1016/S1003-6326(16)64460-6.
[16] Ostrovski O, Zhang G, Kononov R, Dewan MAR, Li J. Carbothermal solid state reduction of stable metal oxides. Steel Res Int 2010;81:841–6. https://doi.org/10.1002/srin.201000177.
[17] Dang J, Zhang G-h, Chou K-c. Kinetics and mechanism of hydrogen reduction of ilmenite powders. J Alloys Compd 2015;619:443–51. https://doi.org/10.1016/j.jallcom.2014.09.057.
[18] Dang J, Chou K-C, Hu X-J, Zhang G-H. Reduction kinetics of metal oxides by hydrogen. Steel Res Int 2013;84:526–33. https://doi.org/10.1002/srin.201200242.
[19] Dang J, Zhang G-h, Hu X-j, Chou K-c. Non-isothermal reduction kinetics of titanomagnetite by hydrogen. International Journal of Minerals, Metallurgy, and Materials 2013;20:1134–40. https://doi.org/10.1007/s12613-013-0846-9.
[20] Pang J-m, Guo P-m, Zhao P, Cao C-z, Zhao D-g, Wang D-g, et al. JIJoM, Metallurgy Reduction of 1-3 mm iron ore by H2 in

a fluidized bed. International Journal of Minerals, Metallurgy and Materials 2009;16:620–5. https://doi.org/10.1016/S1674-4799(10)60002-7.
[21] Winter C-J. Hydrogen energy—abundant, efficient, clean: a debate over the energy-system-of-change. Int J Hydrogen Energy 2009;34:S1–52. https://doi.org/10.1016/j.ijhydene.2009.05.063.
[22] Zhao Y, Fjiecr Shadman. Reduction of ilmenite with hydrogen. Ind Eng Chem Res 1991;30:2080–7. https://doi.org/10.1021/ie00057a005.
[23] Vijay P,L, Venugopalan D Ramani, et al. Metallurgical SJ, Preoxidation and hydrogen reduction of ilmenite in a fluidized bed reactor. Metall Mater Trans B 1996;27:731–8. https://doi.org/10.1007/BF02915601.
[24] Yu J, Hu N, Xiao H, Gao P, Sun Y. Reduction behaviors of vanadium-titanium magnetite with H2 via a fluidized bed. Powder Technol 2021;385:83–91. https://doi.org/10.1016/j.powtec.2021.02.038.
[25] Maria GD, Brunetti B, Trionfetti G, Ferro D. JAIoP. High temperature interaction between H2, CH4, NH3 and ilmenite. American Institute of Physics; 2003. https://doi.org/10.1063/1.1541412.
[26] Wang Y, Yuan Z, Matsuura H, Tsukihashi F. Reduction extraction kinetics of titania and iron from an ilmenite by H2–Ar gas mixtures. JII ISIJ Int 2009;2:164–70. https://doi.org/10.2355/isijinternational.49.164.
[27] Chen F, Lv W, Zhou G, Liu Z, Chu M, Lv X. Investigation of the hydrogen-rich reduction of panzhihua ilmenite concentrate pellets. Journal of Sustainable Metallurgy 2022. https://doi.org/10.1007/s40831-022-00555-3.
[28] Zhang G-H, Chou K-C, Zhao H-L. Reduction kinetics of FeTiO3 powder by hydrogen. ISIJ Int 2012;52:1986–9. https://doi.org/10.2355/isijinternational.52.1986.
[29] Baysal Z, Kirchner J, Mehne M, Kureti S. Study on the reduction of ilmenite-type FeTiO3 by H2. Int J Hydrogen Energy 2021;46:4447–59. https://doi.org/10.1016/j.ijhydene.2020.10.266.
[30] Si X-g, Lu X-g, Li C-w, Li C-h, Ding W-z. Phase transformation and reduction kinetics during the hydrogen reduction of ilmenite concentrate. International Journal of Minerals, Metallurgy, and Materials 2012;19:384–90. https://doi.org/10.1007/s12613-012-0568-4.
[31] Zhang Y, Zhao J, Ma X, Li M, Lv Y, Gao X. Isothermal reduction kinetics and mechanism of pre-oxidized ilmenite. Mining, Metallurgy & Exploration 2019;36:825–37. https://doi.org/10.1007/s42461-019-0075-5.
[32] Salehi H, Seim S, Kolbeinsen L, Safarian J. Phase transitions and microstructural changes during oxidation and reduction of a weathered ilmenite concentrate. Mining, Metallurgy & Exploration 2021;38:1167–73. https://doi.org/10.1007/s42461-021-00397-9.
[33] Lv W, Lv X, Xiang J, Wang J, Lv X, Bai C, et al. Effect of pre-oxidation on the carbothermic reduction of ilmenite concentrate powder. Int J Miner Process 2017;169:176–84. https://doi.org/10.1016/j.minpro.2017.09.008.
[34] Xiao W, Lu X, Ding W, Li C, Zou X. JRMT. Pre-oxidation and hydrogen reduction of panzhihua ilmenite concentrate. Rare Metal Technology 2014:127–31. https://doi.org/10.1002/9781118888551.ch24.
[35] Lv W, Lv X, Zhang Y, Li S, Tang K, Song B. Isothermal oxidation kinetics of ilmenite concentrate powder from Panzhihua in air. Powder Technol 2017;320:239–48. https://doi.org/10.1016/j.powtec.2017.07.058.
[36] Zhang X, Du Z, Zhu Q, Li J, Xie Z. Enhanced reduction of ilmenite ore by pre-oxidation in the view of pore formation. Powder Technol 2022;405. https://doi.org/10.1016/j.powtec.2022.117539.
[37] Xu Baoqiang, Zhao Ding, Sohn Hong, et al. Flash synthesis of Magneli phase (TinO2n-1) nanoparticles by thermal plasma treatment of H2TiO3. Ceram Int 2018;44:3929–36. https://doi.org/10.1016/j.ceramint.2017.11.184.
[38] Lv W, Lv X, Xiang J, Zhang Y, Li S, Bai C, et al. A novel process to prepare high-titanium slag by carbothermic reduction of pre-oxidized ilmenite concentrate with the addition of Na 2 SO 4. Int J Miner Process 2017;167:68–78. https://doi.org/10.1016/j.minpro.2017.08.004.
[39] Liu J, Zeng J, Sun S, Huang S, Kuo J, Chen N. Combined effects of FeCl 3 and CaO conditioning on SO2 , HCl and heavy metals emissions during the DDSS incineration. Chem Eng J 2016;299:449–58. https://doi.org/10.1016/j.cej.2016.04.132.
[40] Briggs RA, Sacco A. Hydrogen reduction mechanisms of ilmenite between 823 and 1353 K. J Mater Res 2011;6:574–84. https://doi.org/10.1557/JMR.1991.0574.
[41] Zhao P-f, Li G-s, Li W-l, Cheng P, Pang Z-y, Xiong X-l, et al. Progress in Ti3O5: synthesis, properties and applications. Trans Nonferrous Metals Soc China 2021;31:3310–27. https://doi.org/10.1016/S1003-6326(21)65731-X.
[42] Kurokawa H, Yoshimatsu K, Sakata O, Ohtomo A. Effects of phase fraction on superconductivity of low-valence eutectic titanate films. J Appl Phys 2017;122. https://doi.org/10.1063/1.4997443.